Formation and nucleosynthetic evolution of the stars

Autor(en): **Bouvier, Pierre**

Objekttyp: **Article**

Zeitschrift: **Jahrbuch der Schweizerischen Naturforschenden Gesellschaft. Wissenschaftlicher und administrativer Teil = Annuaire de la Société Helvétique des Sciences Naturelles. Partie scientifique et administrative**

Band (Jahr): **161 (1981)**

PDF erstellt am: **23.07.2024**

Persistenter Link: https://doi.org/10.5169/seals-90845

Formation and Nucleosynthetic Evolution of the Stars

Pierre Bouvier

1. Diffuse and Condensed Matter in the Universe

On the cosmical scale, the observable universe reveals itself as a collection of galaxies marking out the ways of space-time. Each galaxy is made up of matter, either condensed into stars or scattered in extensive patches of gas and dust. Several phenomena, namely stellar winds, mass loss by stars, explosive events, bear witness of some conversion of condensed into diffuse matter; on the other hand, how do stars come into existence?

Before answering this delicate question, let us recall here that innumerable stellar models have been built since the middle of the present century, using evermore powerful computing means and increasingly refined input physics, allowing us to follow the history of a star of given mass and chemical composition, starting from initial conditions such as those expected to prevail when nuclear burning is first switched on at the star's centre.

The results given by these model computations, which build the main body of the theory of stellar evolution, have made it possible to ascribe a fairly definite age to any star with known observable characteristics and it soon became clear that the younger bright stars, as we observe them in the galaxies, are most often associated with interstellar clouds of diffuse matter from which they presumably originate. What we find in those clouds in gas, mostly hydrogen often in molecular form, and dust grains.

Data on the masses of clouds come from the observation of the 21 cm hydrogen line, of interstellar absorption lines (due to ionized calcium in particular) and of obscuration caused by dust grains. The mean mass density inside large interstellar clouds should be on the order of 10^{-23} g cm^{-3} (Allen 1973), but our attention will be drawn especially towards some dark dust clouds showing little if any 21 cm emission, so that hydrogen seems to be essentially in molecular form in these fairly dense clouds, which are likely to form stars. The largest values of the density within such clouds are close to 10^{-19} g cm^{-3}.

2. Heating and Cooling Processes

An isolated interstellar cloud is submitted to the effects of two adverse forces: self gravitation which tends to produce a collapse of the cloud towards some central region and pressure forces conversely leading to a dispersion of the cloud in space. Although turbulent motions, magnetic fields and rotation of the cloud might play a significant role in certain cases, we shall generally consider here a pressure of thermal nature only. In order to estimate the temperature of an interstellar cloud, we have to call on some sort of balance between the heating and cooling processes going on inside the cloud.

At densities of 10^{-22} g cm^{-3} at least, we should retain primarily (Larson 1974) the following heating and cooling processes:

1) Heating effects by low energy galactic cosmic rays, ultraviolet radiation, soft X-rays; when, during some contraction, the optical depth of the cloud becomes much larger than unity, and the density larger than 10^{-19} g cm^{-3}, these mechanisms lose their importance to the advantage of compressional heating.

2) Among the cooling processes, the most important appears to be collisional excitation with free electrons and protons, of ions (often CII), atoms (OI), molecules (H_2, CO) followed by infra-red emission of radiation but here again, in very dense and opaque clouds, another process shall prevail, namely cooling due to inelastic collisions of mole-

cules with dust grains, followed by infra-red radiation emission from the grains.
By equating the heating and cooling rates for the gas and dust, one manages to obtain a density-temperature law illustrated in the (log ρ, T) plane for a given mass and given chemical composition of the cloud (Fig. 1). This curve is in fact practically unaffected by a change in the mass of the cloud and, as regards chemical composition, it is sensitive in the lower values of the density range to the assumed abundances of the coolants CII and OI. It is worth noticing here that in the density interval between 10^{-21} and 10^{-12} g cm^{-3}, the temperature varies only slightly, remaining around 5 to 20 K, a result in good agreement with radio observations of the comparative strengths of the 21 cm and Lyα interstellar line absorptions in dark clouds.

3. Gravitational Instability, Fragmentation

If self-gravitation is to dominate over the pressure forces (gravitational instability), the gravitational potential energy of the cloud must, in the context of the virial theorem, exceed twice its kinetic energy.
This condition for collapse, called the Jeans criterion, is expressed in the case of a spherical homogeneous cloud of radius R, mass M, temperature T, by the inequality

$$\frac{3}{5} G \frac{M}{R} > 3 \frac{\mathscr{R} T}{\mu} \qquad (1)$$

where G, $\mathscr{R}$ are respectively the gravitation and the gas constant, μ being the mean molecular mass number of the cloud's medium.
Therefore, in a cloud of given M, T, gravitational instability will occur when

$$R < R_c \equiv 0.2 \frac{GM}{\mathscr{R} T} \mu \qquad (2)$$

To the critical radius R_c corresponds, for a cloud of a given mass density ρ and temperature T, a critical minimum mass M_J, allowing the Jeans criterion to be written also:

$$M > M_J \equiv 5.45\, \rho^{-1/2} \left(\frac{\mathscr{R} T}{G \mu} \right)^{3/2} \qquad (3)$$

Adopting a more realistic approach than that of a mere homogeneous cloud would only slightly modify the numerical factors in (2) and (3).
Turning back to the equilibrium curve of section 2, obtained as a result of heat balance inside the cloud, we may then express M_J as a function of ρ only; thus for a rather typical large interstellar cloud where $\rho \sim 10^{-22}$ g cm^{-3}, the minimum unstable M_J given by (3) is of one thousand solar masses at least. However, the normal range of stellar masses extends from about 0.03 $M_\odot$ to an upper limit which, according to the latest massive star evolutionary models (Maeder 1980) should be taken around 150 to 200 $M_\odot$. Under external conditions of strong compression due either to galactic density waves or to shock waves from a supernova event, M_J could perhaps fall into this upper mass range, but in general, a large interstellar cloud is not likely to collapse and condense into a single normal star. Consequently, fragmentation of the initial cloud is expected, presumably in several steps, the number of these steps being sensitive to the inner motions of the cloud (rotation, turbulence) and also to the combination of atoms into molecules (Reddish 1978).
Replacing in (2) R_c by $R_c = (3\ M/(4\pi\rho_c))^{1/3}$, the Jeans criterion for the gravitational instability of a cloud of given M, T now reads

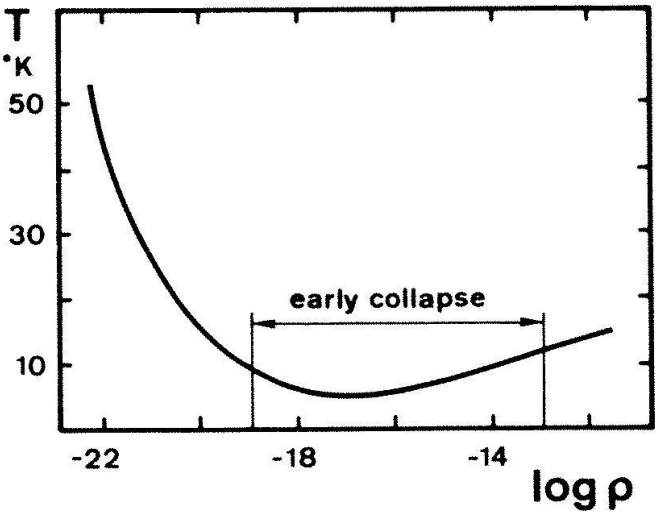

Fig. 1. Equilibrium temperature-density curve resulting from heat balance inside in interstellar cloud (ρ in gcm^{-3}). The density range for which $-19 < \log\rho < -13$ corresponds to the isothermal collapse of a protostar (see text).

$$\rho > \rho_c = \frac{375}{4\pi M^2}\left(\frac{\mathscr{R}T}{G\mu}\right)^3 \qquad (4)$$

If $\rho \gg \rho_c$, the cloud is unstable against fragmentation and tends to break into smaller clouds in which, owing to their smaller masses but nearly same temperature T, the density ρ will get closer to the corresponding critical ρ_c. At the end of the fragmentation process, $\rho = \rho_c$ inside the fragments and the initial large cloud has now become an aggregate of protostars.

The concept of fragmentation agrees well with the observational situation suggesting that most of the stars if not all of them, and especially the more massive ones, are born inside cloud (protostar) aggregates later becoming stellar associations or clusters. In spiral galaxies, the associations and dark interstellar clouds are both found within the spiral arms.

Finally, let us mention that model computations of cloud collapse yield a mass distribution of the ultimate fragments which agrees well with the observed mass spectrum of the youngest stars: the small mass stars are much more numerous than the massive ones and the distribution function f(m) behaves like m^{-2}.

4. Evolution of a Protostar: Isothermal Phase

The Jeans mass M_J given by (3) with the (ρ, T) dependence of Figure 1 is a sharply decreasing function of ρ, going down over the entire range of stellar masses, approximately from 10^2 to 10^{-2} solar masses, as ρ increases from 10^{-21} to 10^{-12} g cm^{-3}. We thus expect protostars to form by fragmentation at minimum density $\rho = \rho_c$ in the former density range and since the corresponding temperature remains, as mentioned at the end of section 2, close to 10 K right up to $\rho \sim 10^{-12}$ g cm^{-3}, the early contraction phase of a protostar will develop in a quasi-isothermal condition.

Numerical computations of the collapse of a spherical protostar are based on the set of Eulerian equations of hydrodynamics together with a mass distribution in spherical shells around the centre. Boundary and initial conditions are not easy to specify; Larson (1974) chose a constant boundary of the protostar (corresponding to an adequate value of the external pressure) and started the computation with a cloud of uniform density $\rho \approx \rho_c$; this avoids having to specify in detail the initial conditions of the protostar, connected to the state reached at the end of the fragmentation phase.

Results obtained with different assumptions and by different authors appear qualitatively similar. Starting with constant ρ and T values (Larson), such as $\rho = 10^{-19}$ g cm^{-3} T $\approx$ 10 K, the pressure will be initially constant throughout the protostar and for lack of a pressure gradient, we find ourselves in the case of an initially freely falling configuration.

A pressure difference shall develop immediately after with the surroundings, at the cloud's surface, and the contraction of the outer layers decelerates, whence the occurrence of a density and of a pressure gradient. Meanwhile the deep interior keeps falling freely at a time-scale t_{ff} proportional to the inverse square root of the initial density. This is also the time needed for the boundary separating the still homogeneous core from

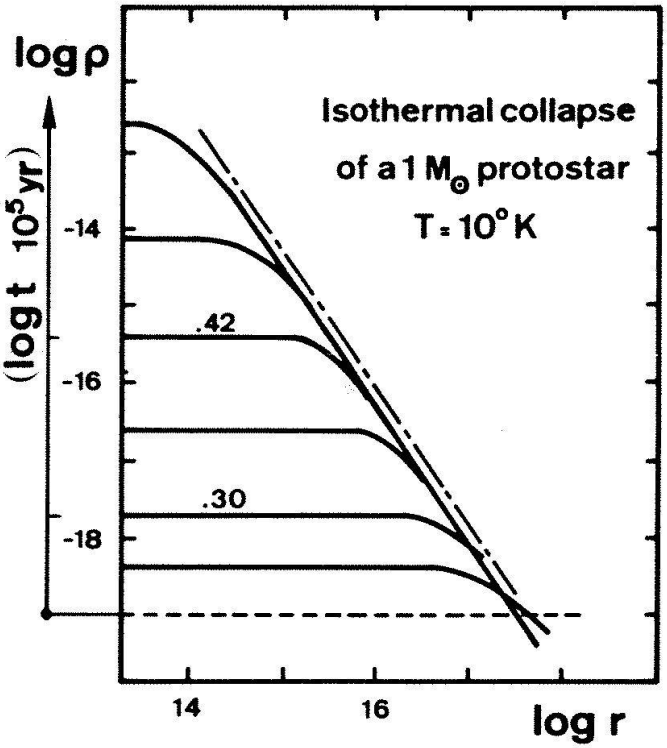

Fig. 2. Density distribution inside a 1 $M_\odot$ protostar at different times during isothermal collapse, starting at t = 0 when logρ = − 19 and ending at t = 300,000 years when logρ = − 13.
The limiting envelope curve follows a $\rho \propto r^{-2}$ law.

the inhomogeneous envelope, to travel inwards with the speed of sound (rarefaction wave). The evolution depicted in figure 2 concerns the isothermal collapse of a spherical non rotating protostar of one solar mass, and initial density 10^{-19} g cm^{-3}; This collapse is highly non homologous, exhibiting an increasingly strong central density peak, while the density profile $\rho(r)$ in terms of the distance r to the centre gradually unfolds according to the law $\rho \propto r^{-2}$.

As we saw in section 2, the cooling processes involved lead to infra-red emission from the grains and this radiation escapes freely from the protostar, which is therefore an infra-red source during isothermal collapse. This picture is in good agreement with observational evidence: infra-red sources have indeed been found in direction of many dark clouds, indicating that some of these clouds are the sites of current star formation. Recently, Snell (1981) has studied the atomic and molecular properties in nine interstellar dark clouds, obtaining a partial mapping of these clouds in infra-red.

The kinetic temperature in the dense regions of the clouds is between 10 and 20 K and their central density on the order of 10^{-19} g cm^{-3}. The relevant clouds have masses of order 10 to 140 $M_\odot$ (which has no bearing on the curves of figures 1 and 2) and exhibit density gradients in which the density, strongly peaked at the centre, diminishes outwardly according roughly to a r^{-2} power law.

The end of the isothermal phase is attained when the central density reaches 10^{-13} g cm^{-3}; the medium then completely absorbs the radiation and a central core appears, heating up rapidly under further collapse.

5. Further Evolution towards the Main Sequence Stage

The protostar now consists of a small very dense core, containing 1% of the total mass, surrounded by an extended rarefied envelope still falling on the core, hence a sharp inward directed velocity gradient quickly steepening into a shock front at the core's surface. The opaque core increases in mass but shrinks in radius by losing energy from its outer layers, while the collapse of its central part is more adiabatic than isothermal, a large fraction of the energy released there being spent in dissociating and further ionizing the former molecular hydrogen. At the end of this short (a few centuries) and rather violent non-isothermal evolutionary step, during which the temperature rises only slowly, the central collapse gets balanced by the pressure forces, and this leads finally to the formation of a second core, termed the stellar core by Larson and having a mass less than 10^{-2} $M_\odot$, a density close to 2×10^{-2} g cm^{-3} and a temperature around 20000 K.

The evolution of the protostar is now characterized by the infall of the outer layers of the protostar on the stellar core, the latter continuing to grow in mass at the expense of the envelope and eventually acquiring the bulk of the protostellar mass.

In the case of fairly low mass protostars ($M < 3$ $M_\odot$), the envelope accumulates on the stellar core while the heating by slow contraction of the core becomes increasingly important as compared to the energy generated by the shock front. After about one million years for a 1 $M_\odot$ protostar, nearly all the envelope has fallen on the core and this 1 $M_\odot$ object has become a visible star (point No 6 on track in figure 3).

In case of a protostar of mass $M > 3$ $M_\odot$, the stellar core evolves more rapidly and the central temperature will soon become high enough for hydrogen nuclear burning to ignite before the infall of the envelope matter has declined to zero. Furthermore, in very massive stars, H-burning produces a strong temperature increase of the core, thus a large radiation pressure at its surface, causing a partial reversal of the infall of the remaining envelope and the ejection of the outer layers, finally leaving a massive main-sequence star. According to these model computations, massive protostars transform directly into main-sequence stars, characterized by core hydrogen burning (Appenzeller 1980).

However, as we just saw before, such is not the case for the lower mass protostars; consider again the 1 $M_\odot$ protostar which, 1.3 million years after the beginning of its collapse, became a visible star. It is now subject to a slow contraction, undergoing a quasi-equilibrium stage during which about half of the energy released is used up in heating the inner region, while the other half is radiated

away. The opacity is quite large, so that the energy is transported inside the star mainly by convection at first; later on, however, the medium gets hotter and less opaque, allowing radiative energy transfer to set up within most of the star.

Accordingly, the point representing the 1 $M_\odot$ star in the HR diagram follows a quasi-vertical path downward (the so-called Hayashi track, HT) and after a luminosity minimum, ascends slowly to the left, with surface temperature and luminosity both increasing (figure 3, points 6′–7). Near the centre, the first nuclear reactions between H and light elements D, Li, Be will rapidly destroy most of the latter and when the central temperature goes beyond 8×10^6 degrees, steady conversion of hydrogen into helium sets in; the 1 $M_\odot$ star has now reached, 50 million years after it came first visible, the main sequence stage where it will spend most of its life, in a state very close to hydrostatic and thermal equilibrium (point 8).

The larger the masses, the shorter the evolutionary timescales; thus for a 3 $M_\odot$ star the time for H burning to settle is around 2 million years, which is comparable to the accretion time for the envelope to fall on the stellar core. A 5 $M_\odot$ protostar will become, only after 500 thousand years, visible as a main-sequence star but H-burning had started already 100 thousand years earlier in the core.

In all the former considerations, we had neglected rotation effects which might indeed alter significantly the stellar evolution. Many investigations are presently on the way, with more elaborate computing codes. Let us just mention a recent paper by Regar and Shaviv (1981) who studied collapse and star formation processes in rotating turbulent interstellar gas clouds, without assuming a mechanism for the transport of angular momentum. It seems likely that the collapse with turbulent viscosity leads to the formation of a central protostar surrounded by a disk when the rotation is low enough and the turbulence efficient, but in the present treatment of the problem, it cannot yet be concluded that one reaches the state where a central star is formed, together with a planetary system. When the rotation is fast or turbulent transport less efficient, the central opaque object is very flat and this raises the possibility of multiple star formation.

Anyway, the picture of protostar evolution outlined above still remains somewhat controversial; new very recent infra-red mappings of the large Orion molecular cloud complex reveal that the compact infra-red

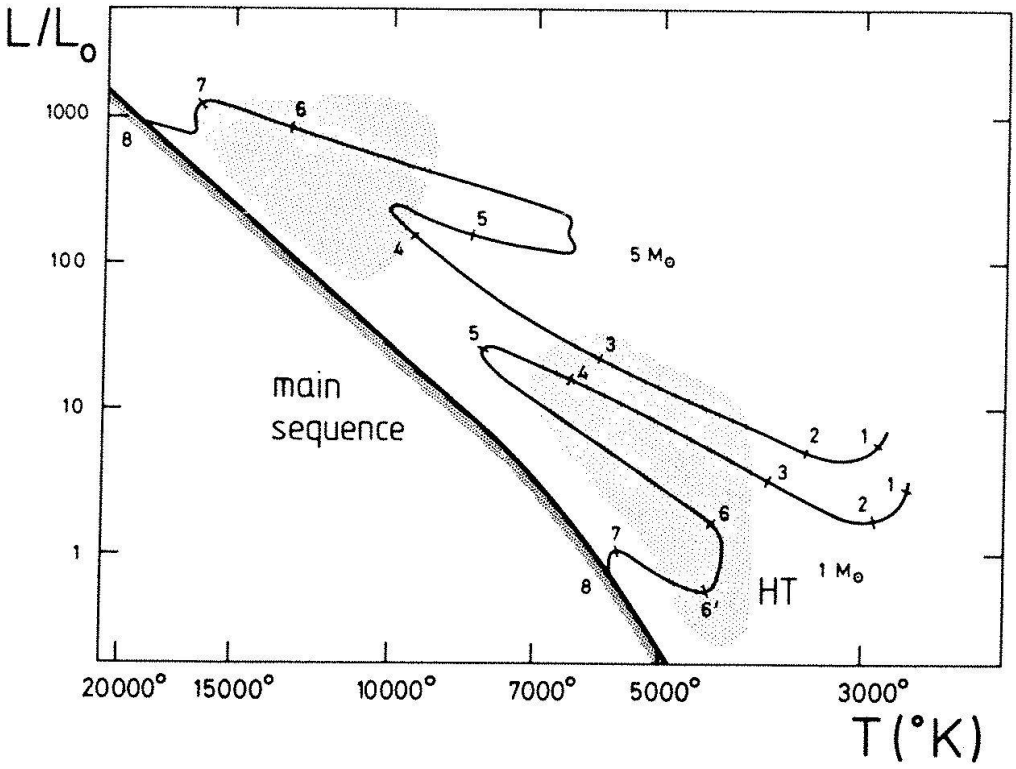

Fig. 3. Evolution of a 1 $M_\odot$ and a 5 $M_\odot$ protostar towards the main sequence. Numbers along tracks refer to specific evolutionary stages; it is a point No 6 that the protostar becomes a visible star. The upper shaded area denotes the Herbig Ae stars and the lower one the T Tauri stars.

objects thought at first to be protostars might well consist of very young and massive stars, dramatically shedding matter in the form of a dense stellar wind (Wynn-Williams 1981).

6. The Main Sequence as the First Nuclear Burning Stage

On account of the low potential barrier of its nucleus (1.4 MeV) and further of its cosmically preponderant abundance, hydrogen appears as the first major nuclear fuel met in stellar interior conditions. Consequently, a star spends most of its life in the narrow band of the colour-luminosity diagram termed the main-sequence, starting from its lower envelope and moving slowly upwards. If we follow the main-sequence from right to left, we pass from the lower to the higher mass stars (figure 4). The time spent in the main-sequence stage is shorter for the massive stars, since the thermonuclear reactions are enhanced in a hotter environment; if a one solar mass star stays about 10 billion years in the main-sequence, the lifetime drops to 10 million years for a 15 $M_\odot$ star.
The H-burning reactions occurring in stars, converting H into He are of two kinds: the proton-proton chains and the CNO cycles (first investigated at the end of the thirties by C.F. von Weiszäcker and H.A. Bethe). The p-p chains dominate in cool stars; of these three chains, the first can operate from pure hydrogen, while the two others work with ^{4}He as a catalyst. On the other hand, the CNO cycles require the presence of catalytic isotopes of carbon, nitrogen, oxygen and are more efficient in hotter stars. On the approach to an equilibrium state, these C, N, O isotopes have their initial abundances modified, and when the equilibrium temperature is attained (for instance 25 million degrees for a central density of some 100 g cm^{-3}), the most abundant of these isotopes is ^{14}N.
Anyway, the main outcome of this main-sequence stage is the nucleosynthesis of helium from hydrogen within the stellar core. The energies liberated by these thermonuclear reactions in the central regions of the main-sequence stars have enabled us, fixing a suitable chemical composition of the stellar matter, to account for the observed luminosities of these main-sequence stars in a most satisfactory way.

7. The Red Giant Stars as Second Nuclear Burning stage

When hydrogen is exhausted in the stellar core, a gravitational contraction of the core follows, together with a wide expansion of the outer envelope: in the colour-luminosity diagram, the representative point of the star moves far away to the right of the main-sequence and the star has now become a red giant (figure 4), with high luminosity, large radius and a deep convective envelope. The central temperature has now risen beyond 120 million degrees, favouring the ignition of helium-burning through triple α-process, where three ^{4}He nuclei react together simultaneously, to form a carbon nucleus ^{12}C. When enough ^{12}C is present, further α-capture by ^{12}C can synthesize oxygen ^{16}O, while ^{14}N resulting from the CNO cycles which still operate in a H-burning shell source outside the He core may also react with ^{4}He to give some ^{18}O.
At the end of such reactions, about 2% of ^{18}O has been formed (starting with a standard chemical composition for population I stars), which is enough to induce further reactions with α particles, releasing free neutrons, important for the later building of elements heavier than those of the iron group.
The core He-burning phase (together with a shell H-burning) lasts five or six times less than the core H-burning on the main-sequence; the end products are now carbon, oxygen, and some neon, magnesium. The reaction rate of the C($\alpha\gamma$)O reaction contains uncertain parameters, so that we may always adjust the C and O abundances resulting from the He-burning to the observed values; on the other hand, the long lifetime of ^{16}O against α-capture makes it impossible, through O(α, γ)Ne, to obtain as much ^{20}Ne as ^{16}O as the observations seem to require.

8. Carbon and Oxygen Burning Stages

Stellar evolution followed hitherto has proceeded through two successive hydrostat-

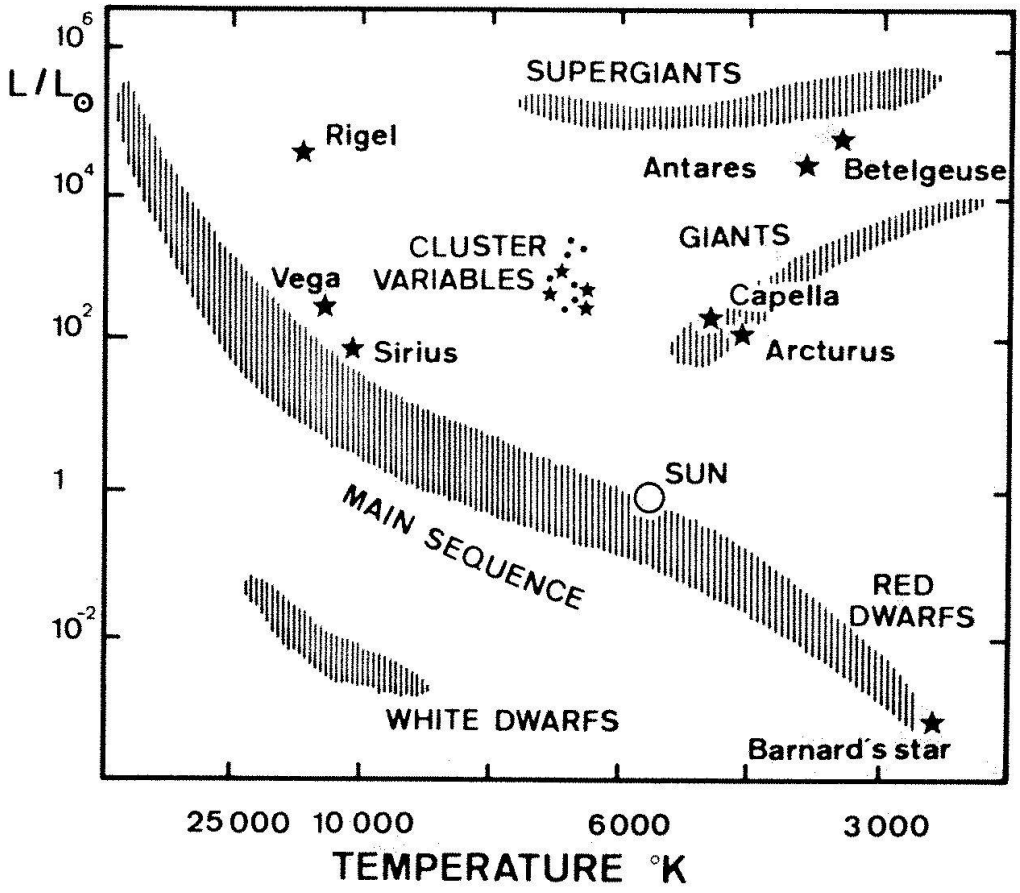

Fig. 4. Qualitative Hertzsprung-Russell Diagram.

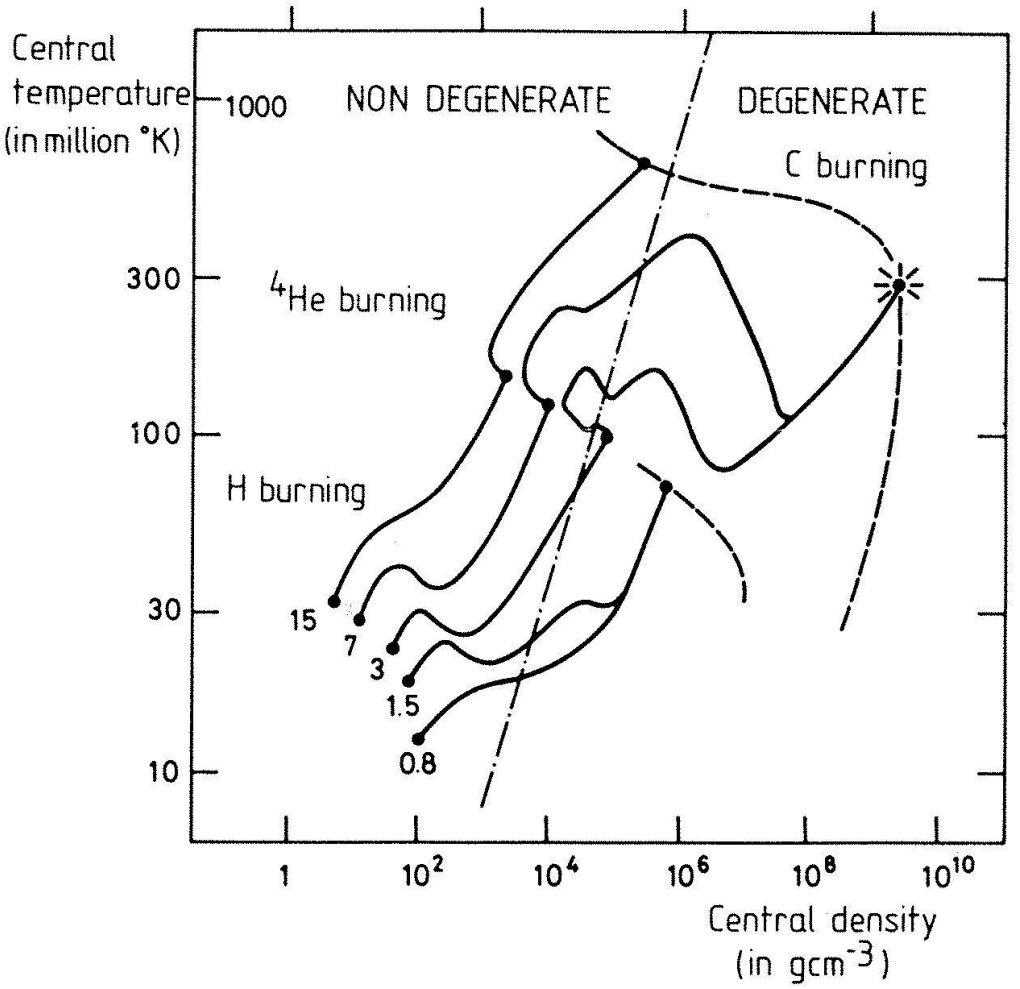

Fig. 5. Central conditions inside stars of masses ranging from 0.8 to 15 $M_\odot$ evolving from main sequence to carbon ignition. The dash-dotted line separates roughly the degenerate and non-degenerate regions of the (logT, logρ) plane.

ically stable nuclear burning stages, separated by a gravitational contraction of the star's core. Similarly, further hydrostatic nuclear burning stages, first examined by G.R. Burbidge, W.A. Fowler, F. Hoyle more than 20 years ago, can occur inside very hot and massive stars, located in the supergiant region of the colour-luminosity diagram (figure 4). When the temperature T rises beyond half a billion degrees K under the contraction following the helium-burning phase, the carbon nuclei will start to react between themselves and due to the high excitation of the compound nucleus ^{24}Mg associated to the reaction $^{12}C + ^{12}C$, we are faced with several outgoing channels, the two most probable being $^{23}Na + p$ and $^{20}Ne + \alpha$. At the typical temperatures of 600 to 700 million degrees required for this carbon-burning stage, the liberated p (protons) and α-particles are rapidly recaptured, eventually yielding free n (neutrons) through subsequent reactions like $^{12}C(p,\gamma)^{13}N(,\beta^+\nu)^{13}C(\alpha,n)^{16}O$. Such free neutrons are also produced by the channel $^{12}C + ^{12}C \rightarrow ^{23}Mg + n$, which is endothermic and much less probable than the two former ones.

Anyway, at the end of the preceding reactions, ^{24}Mg being the most stable of all the nuclei involved, becomes the most abundant product element of carbon burning.

If ever T attained a billion degrees, the oxygen-burning may set in and, similarly to the case of carbon, the $^{16}O + ^{16}O$ reaction has two prominent outgoing channels, yielding respectively free p's and free α's while a third, less important one, produces free n's.

Here, as a result of the relevant O-burning reactions, isotope ^{28}Si, the nucleus of which is the most stable among all those involved, becomes the most abundant product element of oxygen-burning.

9. C-Detonation

In the course of stellar evolution, the central conditions exhibit increasing densities and temperatures; therefore electron degeneracy sets in, and fairly soon for low mass stars (figure 5). At 0.6 billion degrees, neutrino emission due to universal weak interaction processes becomes significant and further, around a billion degrees, half the energy radiated by the star is in form of neutrinos. The subsequent cooling of the C–O degenerate core tends to render the latter still more degenerate, thereby postponing the ignition of carbon. The situation is now similar to the one met in the degenerate helium core of a less massive star at the end of its core hydrogen-burning phase: the ignition of helium leads to the so-called He flash which mixes somewhat certain inner layers without destabilizing the whole star which goes on evolving to the final white dwarf stage, after undergoing significant mass loss.

But in the very hot and dense environment ($T \sim 0.6 \times 10^9$ K, $\rho \sim 10^9$ g cm^{-3}) reached in the degenerate centre of a supergiant star, the ignition of carbon entails an explosive C-detonation blowing up the star entirely.

Such an evolution should be envisaged for stars of moderate mass, say between 3 and 8 solar masses $M_\odot$ although the complete absence of a dense remnant (like a pulsar) after the explosion probably discards this scenario as an explanation of a supernova event.

Below $M = 3\ M_\odot$ nuclear burning stops, as we just saw, at the He-flash and no further nucleosynthesis will occur. Further, in very small mass stars ($M < 0.1\ M_\odot$), degeneracy sets in before the firing of any nuclear reaction. On the other hand, C-ignition inside a massive star (more than $8\ M_\odot$) can take place in nondegenerate matter, eventually followed later by O-burning. The massive stars (around $22\ M_\odot$) develop an inner composite structure consisting of an iron nucleus, surrounding by concentric layers successively enriched mainly in Si, Ne, ^{16}O, ^{12}C, ^4He, H (onion-skin structure) (figure 6). Nuclear burning goes on at the inner interfaces between contiguous layers.

10. Photodisintegration. Silicon Melting

Between 1 and 2 billion degrees, the photodesintegration of nuclei by the radiation of the fantastically hot photon bath will set in (comparable, on another scale, to photoionization of atoms occurring around 10 thousand degrees), thus excluding the possibility of new hydrostatic nuclear burning phases of the fusion type seen before.

The less stable nuclei (like those of odd

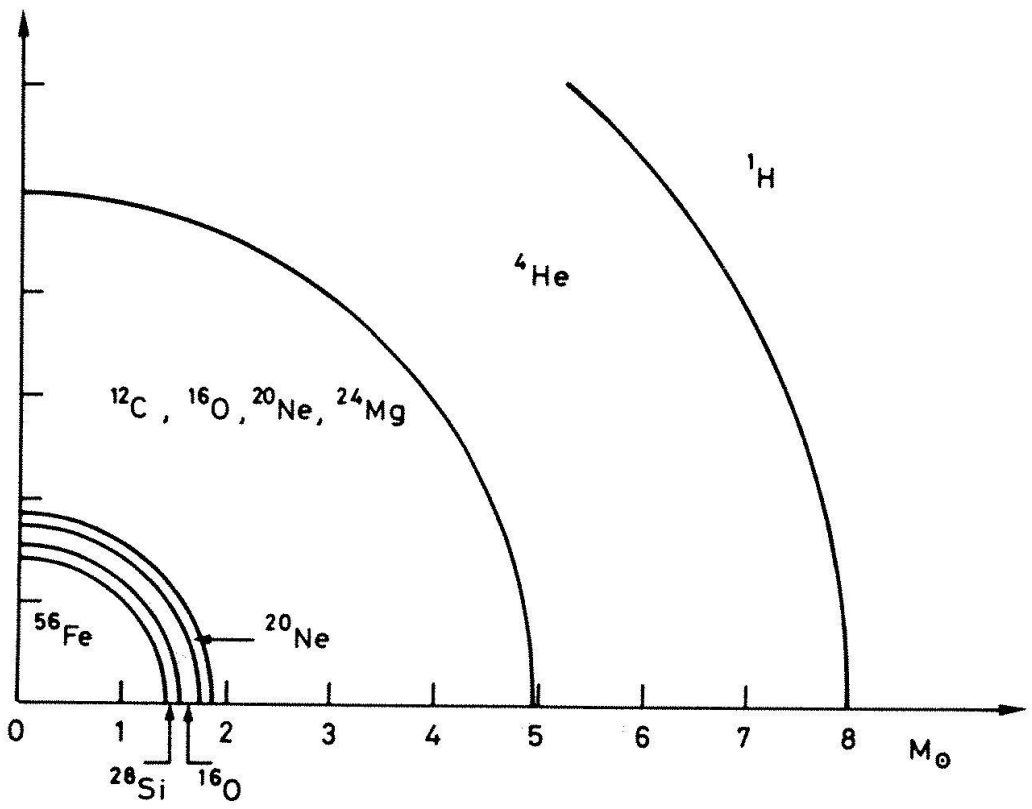

Fig. 6. Internal structure of a massive star (around 22 $M_\odot$) having presumably reached the pre-supernova stage. The composition of the successive concentric layers reflects the successive nuclear burning stages.

atomic mass number) shall be destroyed in favour of more stable ones, so that photodisintegration tends to redistribute the ejected loosely bound nucleons (α, p, n) into nuclei where they become more tightly bound.

In the range of the relevant intermediate nuclear masses, ^{28}Si is the most stable nucleus against photodisintegration and when it starts to be photodisintegrated, at temperatures drawing close to 3 billion degrees, many reactions of type (α,γ), (p,γ), (n,γ) and their inverses are at work.

The nucleons slowly photoejected by ^{28}Si are principally recaptured by ^{28}Si nuclei (which are the most abundant): reactions like $^{28}Si(\alpha,\gamma)\,^{32}S$ will quickly be partly counteracted by the inverse $^{32}S(\gamma,\alpha)^{28}Si$, but the α-particles ejected by the overwhelmingly numerous ^{28}Si nuclei will also lead to the gradual building of heavier nuclei, through $^{32}S(\alpha,\gamma)$ ^{36}Ar etc in a slow progression towards stabler nuclei, up to those of the iron group which are known to have the maximum binding energies per nucleon. The rates of these photodisintegration and capture reactions being much larger than the rate of variation in elemental abundances, we therefore have here a kind of quasi-equilibrium state of the medium, during which ^{28}Si slowly melts away.

The characteristic time for the photodisintegration redistribution of the nuclei from silicon to the iron group is governed by the photodisintegration rate of ^{28}Si, which itself depends sharply on the temperature T. Remember also that the most tightly bound nuclei in the iron group are not those with equal numbers Z of protons and N of neutrons, but these having a neutron excess by 2 or 4.

When T is around 3 billion degrees, this redistribution time is on the order of one day, which allows β decays to occur so that one reaches the iron group with isotope $^{56}_{26}Fe$ $(Z < N)$, but for T between 4 or 5 billion degrees, no such decays have time to appear and we finally attain isotope $^{56}_{28}Ni$ $(Z = N)$, or $^{54}Fe + 2p$ for still larger T's.

As ^{28}Si disappears, we reach a statistical equilibrium of the medium, in which the abundance of each nuclear species finally depends on the density and temperature of the medium, together with the ratio of the total number of protons to the total number of the neutrons (bound and free, in a given volume).

Independently of the photodisintegration process, the chemical elements of mass number $A \gtrsim 65$, located beyond the iron-group, are less stable on account of their high inner

Coulomb repulsion; they cannot be built by fusion but only by neutron capture as we shall see later (section 14).

11. Abundances of the Elements in the Universe

The well known Standard Abundance Distribution (SAD) curve gives, in terms of the atomic mass number A (figure 7) the relative abundances of the chemical elements as they have been determined in the carbonaceous chondrite meteorites, in the solar and many stellar atmospheres; furthermore a large number of stars and of galaxies follow the SAD curve, as well as the interstellar matter. H and He are by far the most abundant observed elements and when A increases, the abundances decrease sharply before rising again to the iron group ($50 \lesssim A \lesssim 65$). We shall come back later to the light underabundant elements Li, Be, B (section 15) and to the heavy elements (section 14).

We notice further the presence of several peaks in the range of heavy elements, corre-

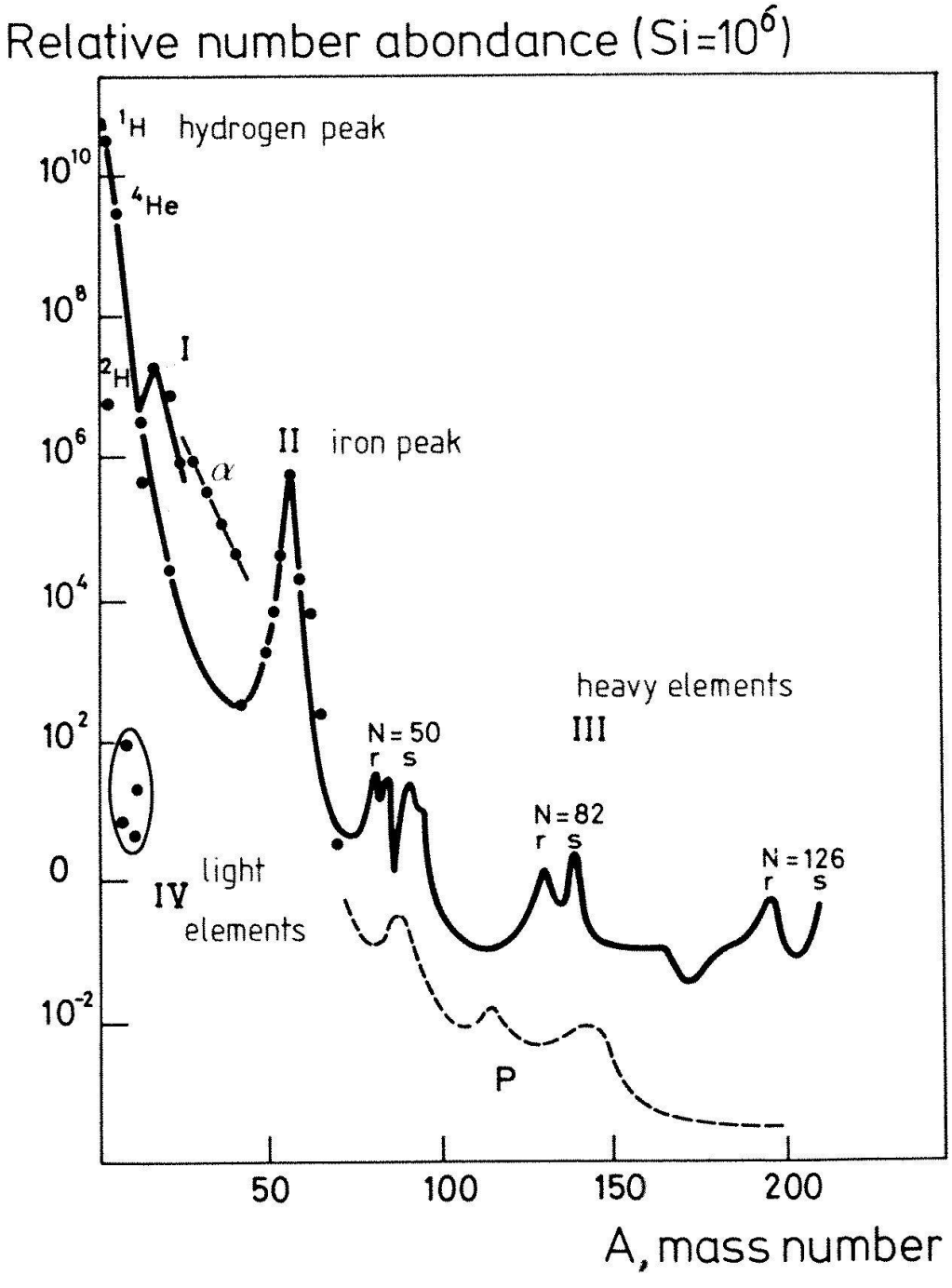

Fig. 7. Standard Abundance Distribution of the Elements (see text).

sponding to the so-called magic nuclei ($N = 50, 82, 126$) for which the n-capture cross-section shows a significant minimum.
The labels s, r, p in Fig. 7 refer to heavy elements formed respectively by the s-, r- or p-processes (section 14).
In order to compare the products of nucleosynthesis which took place deep inside the stars with the data collected in the SAD curve and referring to observations made on the solar system, the solar and stellar surfaces, the interstellar matter, we must consider the possible ejection of the inner nucleosynthesized stellar layers into the outer galactic medium. Let us therefore turn our attention to explosive objects.

12. Explosive Events

Among the known stellar explosive objects, the supernovae are undoubtedly the most conspicuous and powerful, exhibiting a very sudden increase in luminosity followed by a steep and more or less regular decrease of their light curves. The mechanism that triggers a supernova explosion must be able to release a tremendous amount of energy (around 10^{51} ergs) and also to allow the formation of a remnant star.
Recalling the evolution of massive stars ($M \gtrsim 8\ M_\odot$) mentioned at the end of section 9, we saw that these stars acquire an onionskin structure made up of concentric shells, the outermost one containing essentially hydrogen, while the internal layers appear to be successively enrichted in He, C, O, Ne, Si as a result of the different hydrostatic nuclear burning stages which they underwent (figure 6). In the central Fe-Ni core, the temperature now tends to exceed 5 billion degrees, while contraction favoured by the cooling effect of a strong neutrino emission accelerates the star's final evolution. However, at such high temperatures photodisintegration of the iron group nuclei becomes possible, leading to

$$^{56}\mathrm{Fe} + \gamma \leftrightarrows 13\,^{4}\mathrm{He} + 4\mathrm{n} - \mathrm{Q}$$

and similar reactions with ^{54}Fe, ^{56}Ni. Since these nuclei are particularly stable, such reactions are highly endoenergetic (large $Q > 0$) therefore capable of triggering a violent implosion of the stellar core, immediately followed by the explosion of the surrounding matter still undergoing nucleosynthetic processes. The central core, which will very quickly be neutronized, finally transforms either into a neutron star or pulsar if its mass is below about $2\ M_\odot$, or otherwise eventually into a black hole. The mechanism just outlined might explain the supernova II phenomenon, observed in galaxies with population I stars.
Much less important with respect to the amount of energy released (10^{43} ergs), are the novae outbursts, which may last quite as long as a supernova event (a few months) but are much more frequent and often recurrent. Without entering here into details (see Audouze and Vauclair 1980), we notice that the nova phenomenon affects only the outer layers of a prenova star, which is probably a white dwarf enriched in C, N, O isotopes. When such a white dwarf finds itself belonging to a binary system, the other companion being a star evolved to the red giant stage, matter from this companion, essentially H and He of its outer layers, is transferred to the white dwarf and heats its surface to 100 million degrees or more, thus triggering the so-called hot CNO cycle and causing a nova outburst, likely to be the site for the formation of some rare odd-A isotopes such as ^{13}C, ^{15}N, ^{17}O.

13. Explosive Nucleosynthesis

The thermonuclear reactions causing the explosive events described in section 12 arise on a much shorter time scale (a few seconds or hours) and at much higher temperatures and/or densities than during hydrostatic stable nuclear burning. The problem, first tackled by W.D. Arnett and J.W. Truran about 12 years ago, is very complicated in general, since we have to follow the abundance variation of many nuclear species through a fairly large network of reactions; moreover the rapidity of the reactions in the present environment renders all the more important their dependence on density and temperature with time, actually involving a hydrodynamic treatment of the explosive process. In attempting to describe such a treatment, we should use the equations of

state and of energy transport within the stellar medium.
Relevant calculations have been performed for some novae outbursts, but not yet for supernovae explosions, where one usually relies on simplifying assumptions. One first assumes that ρ and T evolve according to a theoretical profile for which the characteristic time is the free fall time scale $t_{ff} = 446\ \rho_0^{-1/2}$ as expressed (in cgs units) in the collapse of a uniform gas sphere of initial density ρ_0.
We then write

$$\rho(t) = \rho_0 \exp\left(-\frac{t}{t_{ff}}\right),$$

$$T(t) = T_0 \exp\left(-\frac{t}{3\,t_{ff}}\right)$$

by assuming further the medium (submitted to a strong shock wave) to undergo an adiabatic transformation.
Now, the initial values ρ_0, T_0 are connected by equating the characteristic life-time $t_c(\rho_0, T_0)$ of the relevant nuclear fuel as obtained in usual hydrostatic conditions, to the free-fall time scale $t_{ff}(\rho_0)$; the point is then to compare the possible (ρ_0, T_0) values to the density and temperature attained, during the evolution of a massive star ($22\ M_\odot$) in the different layers (figure 6) just before the supernova explosion.
Thus, for the couple of initial values $(\rho_0, T_0) = (10^5, 2)$ in gcm^{-3} and billion K respectively, explosive ignition of carbon could take place; the ρ_0 value agrees indeed with that met in the C-rich layer of the $22\ M_\odot$ presupernova star while T_0 is a little below the T-value prevailing in that layer.
The same can be said about explosive oxygen burning at $(\rho_0, T_0) = (2 \times 10^5, 2.6)$ and explosive silicon burning at $(\rho_0, T_0) = (2 \times 10^7, 4.7)$.
The final output of explosive nucleosynthesis is very sensitive not only to the (ρ_0, T_0)-values, but also to the initial chemical composition currently parametrized by the neutron enrichment factor $\eta = (N - Z)/(N + Z)$.
The resulting scenario for a supernova event is then the following: the strong shock, induced by the core's implosion due to iron photodisintegration, propagates rapidly outwards through the successive Si-, O-, C-, He-rich layers of the massive star, heating them to bring their temperature (main parameter) at the T_0 value, thereby switching on the corresponding explosive nuclear burning in a very short time.
D.N. Schramm and W.D. Arnett showed that when such exploding stars have expelled all the layers surrounding their dense inner iron core, one does obtain the relative abundances of the elements (at least those with α-nuclei) observed in the solar system. In reality, the presolar interstellar medium has been enrichted by stars which had different masses, but on the average, the nucleosynthesis output appears to be satisfactorily represented by the contribution of a $22\ M_\odot$ star (Schramm 1977).

14. The Formation of the Heavy Elements

As recalled at the end of section 10, the heavy nuclei found beyond those of the iron group ($A > 65$) can no longer be formed by thermonuclear fusion reactions between charged particles; the very high potential barrier of these nuclei becomes insuperable and the only mode of formation for such heavy elements is through neutron capture.
In the (N, Z) plane, where Z is the number of protons and $N = A - Z$ the number of neutrons per nucleus, the known stable heavy elements are located along a curve corresponding to the so-called 'valley of stability' in the (M, Z, A) space, where M is the mass of the (Z, A) nucleus (figure 8).
Adding more and more neutrons to a given nucleus will in general remove it from the curve, in a zone of instability, from which it tends to fall back into the valley of stability through a Z-increase, namely a radioactive decay.
In contrast with fusion reactions, the cross section $\sigma(v)$ for capture of neutrons having velocity v, decreases with energy and in the astrophysical environment met here, the average product $\langle \sigma v \rangle$ giving the rate of neutron absorption, is roughly independent of energy; consequently the life-time t_n of a heavy nucleus against neutron capture is inversely proportional to the neutron density.
The building rate of a heavy nucleus by n-capture depends on the ratios of t_n with the

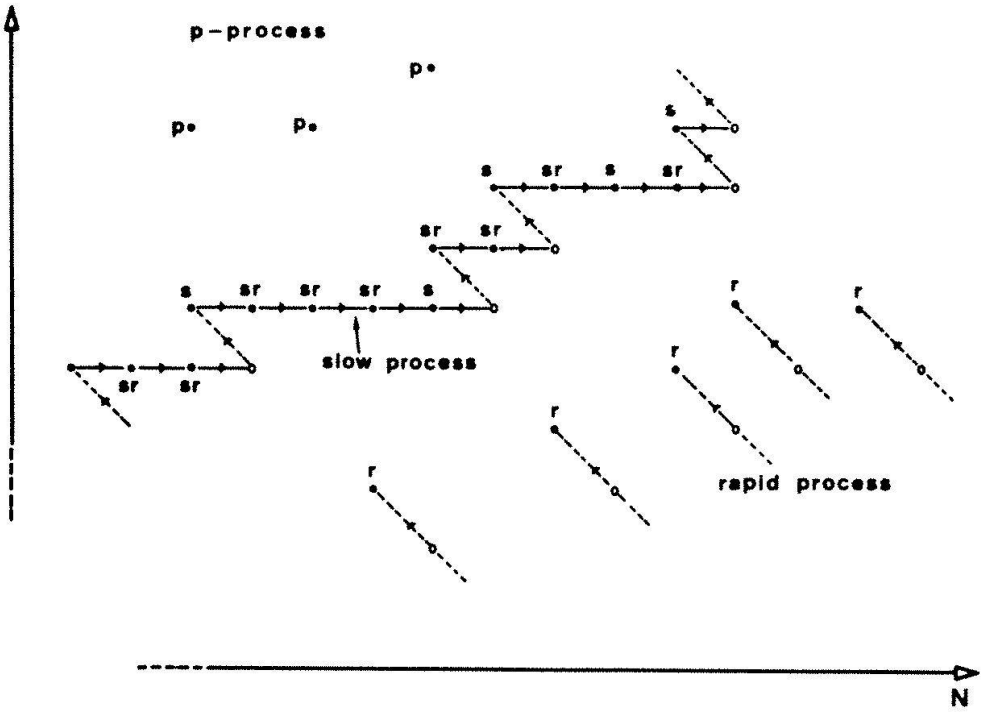

Fig. 8. Schematic illustration of the heavy element building processes in the (Z,N) plane. Full circles denote stable elements; those labelled s,r,p, correspond to the respective s,r,p-processes with produced them and for those labelled sr, formation can occur either by s- or by r-process. Open circles denote β-unstable elements.

average period t_β of β-decay; this ratio is usually much larger or much smaller than unity. In the first case, we are faced with the s-process, where the free neutron flux is sufficiently weak to allow β-decays to occur, but in the second case the n-flux is very intense, no β-decays have time to appear and we get the r-process.

The s-process is assumed to take place during the red giant stage of stellar evolution, in particular when helium flashes induce an incomplete mixing of the H and He zones; ^{12}C resulting from the He-burning may become more abundant than H in the mixed matter, where the CNO cycle reactions then reduce to $^{12}C(p\gamma)\ ^{13}N(,\beta^+\nu)^{13}C$ and ^{13}C can react with He, according to $^{13}C(\alpha,n)^{16}O$ which is an important source of free neutrons. In the He-burning region, the former presence of ^{14}N can also, by α capture and subsequent steps, lead to the release of free neutrons.

The iron-group nuclei are usually considered to be the seed nuclei for the s-process, allowing the gradual building of heavier nuclei from ^{56}Fe to ^{206}Pb; the main property emerging here is the continuous decrease, with increasing A, of the product σN of the cross-section for n capture by nuclei of mass A, times their concentration N.

Observationally, the working of the s-process in stars is illustrated by the presence of Tc (A = 99), detected in the atmosphere of certain red giant stars; this element has indeed been formed in the star, since its radioactive lifetime of 10^5 yr is much shorter than the age of the star.

Moreover the variable star FG Sagittae, to which much attention has been paid lately, revealed a large annual increase in the abundances of s-process elements like Ba, Y, Zr; a similar increase of rare earth s-process elements has been noticed in CI Cygni.

In contrast to the fairly smooth dependence of σN on A in the s-process, yielding a curve in good agreement with the solar values pertaining to s-process abundances, the r-process leads to quite a disorderly picture for σN in terms of A.

The r-path in the Z,N plane brings us far to the right of the valley of stability, viz. to very high n-rich and unstable nuclei (figure 8). As more neutrons are added to the (Z,A) nucleus, a point (Z,A′) is reached, where A′ is distinctly larger than A, beyond which the nuclear binding energy is too weak to allow further n-capture; at this so-called waiting point, the nucleus is subject to no reaction until a β-decay changes Z into Z + 1, so that n-capture may go on for the (Z + 1,A′) nucleus.

It is the poor knowledge about the binding energy of very n-rich nuclei not observed in nature, that makes the r-process not yet fully

understood, but nevertheless, this process appears quite necessary to account for the formation of elements heavier than ^{206}Pb, like Th, U, Pu.

Finally to the left of the valley of stability, we find p-process elements disclosing a proton excess, therefore impossible to be formed by n-capture. Several mechanisms have been proposed to explain their formation; all of them are connected to the s- and r-processes and we shall not go into detail here (see Audouze 1980). Recently, a nucleosynthetic process involving rapid p-capture has been identified in a study on explosive H-burning (Wallace and Woosley 1981); this so-called rp-process has significant implications for element synthesis and energy production in H-rich material at high temperatures; substantial enrichment occurs in elements heavier than oxygen.

15. A Glance at the Light Elements. Spallation Reactions

The light elements D, Li, Be, B are destroyed in stars by p-capture occurring when the temperature exceeds already a million degrees K; they are therefore not produced by stellar nucleosynthesis. On the other hand, He is formed in stars during the main sequence stage (section 6) but not in sufficient amount to account for the observed He in the universe. We have to resort to other nucleosynthetic processes to explain the presence of these light nuclear species, and since the aim of the present lecture was to concentrate on nucleosynthesis in course of stellar evolution, we shall remain satisfied by giving here only a very brief outline about these other processes, of which we retain essentially two: spallation reactions and primordial cosmological nucleosynthesis, described in section 16.

In a spallation reaction, a heavy or intermediate mass target nucleus is hit by a very high energy ($E > 10MeV$) incident particle (p or α) and subsequently broken into several fragments. These reactions are very endoenergetic; f. ex., the following one, studied in laboratory,

$$p + {}^{12}C \rightarrow {}^{6}Li + 3n + 3p + p' + Q$$

requires a threshold energy $E_T = -Q = 30$ MeV. Note that p′ is the incident projectile p with a different energy.

A spallation reaction is usually described by a 2-step procedure: first, when crossing the target nucleus, the incoming p collides with a few nucleons which in turn generate more collisions (cascade) and some of the nucleons have enough energy to leave the target nucleus with the incident $p \rightarrow p'$. After this rapid step ($\lesssim 10^{-21}$sec), the resulting excited nucleus will dissipate its energy more slowly (10^{-16}sec) by evaporating a few more nucleons.

This scheme (Serber model) accounts for the behaviour of the spallation cross-section $\sigma(E)$ which, according to experimental measurements, increases with energy E up to a maximum before decreasing to an asymptotic value, the more sharply the lower the threshold energy E_T.

It has been suggested by Reeves and others about 10 years ago, that the formation of the light elements Li, Be, B is due to the interaction between the Galactic Cosmic Rays (GCR) and the interstellar medium.

These highly energetic GCR, presumably originating in explosive objects such as supernovae, anyway coming from outside the Solar System, interact strongly with the terrestrial atmosphere before reaching the ground. This GCR flux ϕ appears to be isotropic, time-independent and follows, for the higher energies ($E \geq 2GeV$/nucleon) a power law spectrum $\phi \propto E^{-2.7}$ while at lower energies ($< 1GeV$/nucleon) ϕ is strongly perturbed by the Sun.

As rather conspicuous signatures of the interaction between interstellar medium and GCR, let us mention the following peculiarities in the GCR chemical composition: the ratio of odd Z to even Z nuclei is larger than in the standard abundances (cf. figure 7) and the ratio of the light elements to the medium mass elements is very much (10^4) larger than its value in the universal cosmic abundances. This means that along their path in space, the primary rapid (C, N, O, ...) GCR particles hit interstellar H and He atoms, resulting in spallation reactions creating odd nuclei and light elements Li (in general more ^{6}Li and ^{7}Li), ^{9}Be, ^{10}B, ^{11}B.

On the other hand, it appears quite impossible to explain the observed deuterium

abundance ($D/H \sim 10^{-5}$) in the solar system and neighbourhood by spallation reactions due to cosmic rays.

16. Big Bang Nucleosynthesis

Two basic observational facts, namely the recession of the galaxies and the 2.8 K blackbody background radiation, both point to a very dense and hot initial state called Big Bang, from which the universe has started its present evolution. G. Tammann will come back on the evidence for the Big Bang in his forthcoming lecture.

The basic assumptions on which rests any Big Bang model are the validity of the same physical laws (not depending on gravity) everywhere in the universe and the existence of this very dense and hot initial state of the universe when all particles were in equilibrium. Other more restrictive assumptions have to be made, such as homogeneity, isotropy of the universe and a positive baryon number, in order to define the so-called Standard Model which has served as a framework for the nucleosynthesis calculations initiated by R. Wagoner, W. Fowler and F. Hoyle a decade ago.

Without speculating here about the very first instants of expanding universe, let us recall that 10 seconds after the beginning of the expansion, the universe is thought to have reached the end of the so-called lepton era, when energetic photons (>1 MeV) maintained their equilibrium around 10 billion degrees with light particles (leptons) like electrons, muons, neutrinos, in the presence of some baryons left over from previous hadron annihilation, namely protons and neutrons, in about equal amounts through exchange of leptons. When the temperature sinks below 10^{10} K as the universe continues to expand, the neutrons, more massive, become less numerous than the protons, soon stabilizing at a ratio of about 1 n for 5 p's. Meanwhile, the electron-positron pairs have annihilated, leaving a small remainder of electrons.

The primordial cosmological nucleosynthesis is now ready to take place: the first reaction to retain, namely $n + p \rightarrow D + \gamma$, is still practically reversible above 5 billion degrees, so that no deuterium $D = {}^2H$ is yet really produced. Below that temperature, however, when the age of the universe is close to 3 minutes, there will be enough D obtained for subsequent reactions (already met in the p-p chains of H-burning in stars) to produce ^{4}He, with a little ^{3}He, ^{7}Li. The calculations were carried out assuming, in this very early evolutionary stage, a flat Friedmann model universe submitted to an adiabatic expansion: equilibrium is achieved for any reaction when the reaction rate largely outweighs the expansion rate. After 1000 seconds, the temperature has dropped below 300 million degrees and the density is then too low for any other reaction to proceed; consequently, in a quarter of an hour, D and ^{4}He have reached their equilibrium values and no heavier element can be built.

The ^{4}He abundance in mass, quite sensitive to the values of the n/p ratio and of the expansion rate, is close to 25% in the present conditions of the Standard Model for the Big Bang: this is in good agreement with the overall abundance of helium observed in the universe. Thus, the only nuclear species produced in the primordial cosmological nucleosynthesis are D, ^{3}He, ^{4}He, ^{7}Li and, apart from ^{7}Li also synthesized in stars, these are precisely those isotopes that neither stellar nucleosynthesis nor interstellar spallation reactions could account for. Finally we should mention as an important result of the former considerations, that deuterium in the Standard Big Bang is produced in sufficient amount to explain the present observed abundance value $D/H \sim 10^{-5}$, only if today's density of the universe does not exceed 5×10^{-31} gcm^{-3} and this points definitely to an open universe (insofar as the neutrinos reveal no significant rest mass).

17. Conclusion

At the end of this condensed survey about star formation and nucleosynthesis, it is worth emphasizing first the still approximate character of the description obtained today and outlined above. The picture of protostar evolution, mentioned in section 5, might soon improve on account of the infra-red measurements presently being carried out on interstellar molecular cloud complexes.

With respect to nucleosynthesis, many uncertainties stand in our way to follow accurately the advanced stages of nuclear burning in stars, and if the chemical element abundances resulting from explosive nucleosynthesis do represent an improvement over the ones deduced from mere hydrostatic burning, in the sense that they appear to reproduce rather successfully the Solar System abundances, we should keep in mind that what we know of the Solar System may not reflect a truly representative sample of the galactic medium.

Moreover, the exact way to describe an exploding star remains badly known and, as regards the cosmological nucleosynthesis, we must remember that its interpretation rests on the Standard Big Bang model, itself subject to many simplifying assumptions and therefore possibly rather far from the real physical universe.

In spite of all these shortcomings, this description outlined here as resulting from the investigations of the last two decades, does not lack a certain majesty; it leads us to face a universe starting in the hot Big Bang initial state with pre-existing radiation, matter and antimatter, expanding then during more than 10 billion years, undergoing various inner modifications, and giving birth to stars and stellar systems.

In consequence of this evolution, it turns out that all the different chemical species composing every bit of matter existing today (including our own bodies!) have originated, in a remote past, inside stars or eventually during the first minutes after the lepton era, when our universe was still in its glowing earliest infancy.

References

Allen, C.W.: 1973, Astrophysical Quantities (3rd ed., The Athlone Press, London).

Appenzeller, I.: 1980, in 'Star Formation' 10th Saas-Fee Course (Ed. Geneva Observatory).

Audouze, J., and Vauclair, S.: 1980, 'An Introduction to Nuclear Astrophysics' (Reidel Pub. Co.).

Larson, R.B.: 1974, 'Fundamentals of Cosmic Physics', V. 1 (A.W. Cameron, ed.).

Maeder, A.: 1980, Astron. Astrophys. 92, 101.

Reddish, V.C.: 1978, 'Stellar Formation' (Pergamon Press, Oxford).

Regar, O., and Shaviv, G.: 1981, Astrophys. J. 243, 934.

Schramm, D.N.: 1977, in 'Advanced Stages in Stellar Evolution', 7th Saas-Fee course (Ed. Geneva Observatory).

Snell, R.L.: 1981, Astrophys. J. Suppl. Series 45, 21.

Wallace, R.K. and Woosley, S.E.: 1981, Astrophys. J. Suppl. Series 45, 388.

Wynn-Williams, G.: 1981, Scientific Amer. 245, No. 2.

Address of the author:

Prof. Dr. Pierre Bouvier
Observatoire de Genève
Chemin des Maillettes
CH-1290 Sauverny (Switzerland)